SUPPLEMENTAL MATERIAL

Title: A unifying theory of carotid plaque disruption based on structural phenotypes expressed at the lumen/wall interface

Supplemental Methods

The workflow for generating computational fluid dynamics models of the carotid bifurcation using patient-specific geometry is described below.

Geometry and meshing

The geometry used for the computational fluid dynamics (CFD) simulation for a given patient was generated using the CT angiogram obtained during preoperative evaluation for a carotid endarterectomy (CEA). CRIMSON software was used to segment the arterial lumen on CT angiogram and generate the 3-dimensional (3D) geometry.[1] The geometry extended from the distal common carotid artery (CCA) and included the carotid bifurcation, the external carotid artery (ECA), and the cervical internal carotid artery (ICA). The 3D geometry was converted to a fine tetrahedral mesh using ANSYS Meshing software. Each tetrahedron had 0.4mm side length, resulting in a total of ~$3x10^5$ elements for each geometry.

Blood viscosity

Blood is a shear-thinning non-Newtonian fluid whose viscosity decreases at high shear rates. These non-Newtonian properties of blood were modeled using the Carreau model, which describes the viscosity η, dependent on shear rate $\dot{\gamma}$, by the following equation:

$$\eta = \eta_\infty + (\eta_0 - \eta_\infty)[1 + \dot{\gamma}^2\lambda^2]^{(n-1)/2}$$

with the following experimentally validated parameters:[2,3] viscosity at zero shear rate, η_0 = 0.022 Pa s; viscosity at infinite shear rate, η_∞ = 0.002 Pa s; relaxation time, λ = 0.11 s; and power index n = 0.392.

Boundary conditions

Blood flow was driven by a time-dependent velocity boundary condition at the CCA inlet. This velocity boundary condition captured the expected triphasic arterial pulsations. The shape of the inlet velocity boundary condition curve, plotted in Fig. S1, was developed by Hoi et al. by averaging velocity profiles in the CCA among older adults using cine phase-contrast MRI.[4] We normalized this curve before scaling it to each patient's peak common carotid velocity, as measured by Doppler ultrasonography. This velocity vector was directed normal to the inlet. This boundary condition was applied uniformly across the inlet surface.

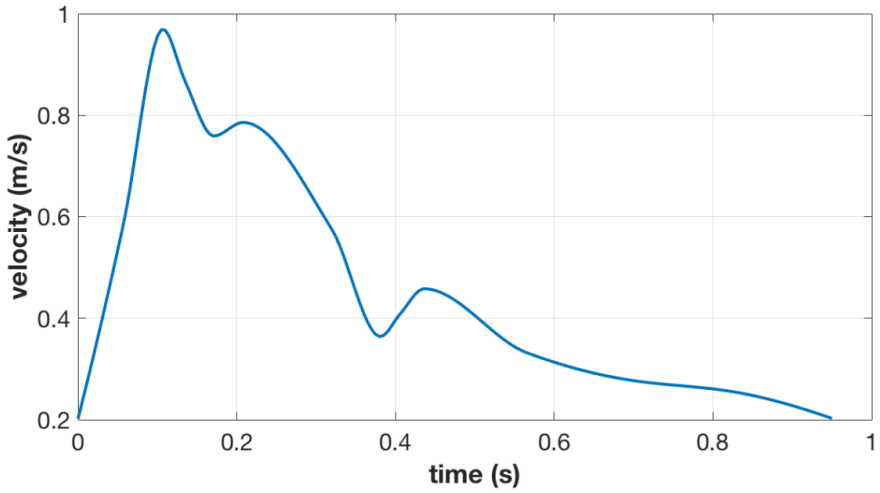

Fig. S1. Time-dependent inlet velocity boundary condition for one cardiac cycle, in a patient with peak CCA velocity 0.97 m/s and heart rate 63 beats per minute.

Outflow boundary conditions were prescribed at the outlets of the ICA and ECA, where flow at the outlet was presumed to be fully developed and extrapolated from the interior.[5] This was preferred over assigning a pressure boundary condition at the outlet, as actual pressure data at the ICA and ECA outlets were unknown. No-slip conditions were applied to the wall of the geometry, which was modeled as a rigid structure.

Solver

A time-dependent numerical solution to the 3D laminar Navier-Stokes and continuity equations was calculated using ANSYS Fluent software. Each time step was solved to convergence every 0.025 second of the cardiac cycle. The third fully solved cardiac cycle was used to plot the flow path lines, the dynamic pressure, and wall shear stress (WSS) distributions over the geometry. The WSS is defined as the magnitude of force per unit area acting tangential to the wall. The dynamic pressure is the force per unit area exerted by the fluid, as a result of fluid flow, and is given by the following equation:

$$P_{\text{dynamic}} = \frac{1}{2}\rho v^2$$

Where ρ is the fluid density and v is the fluid velocity.

Then, we simulated peak dynamic pressure along the wall of the geometry at each timestep of the cardiac cycle (Fig. S2). Interrogating the solution at the height of systole reveals that the peak pressure is 19.6x higher than the average dynamic wall pressure at that timestep.

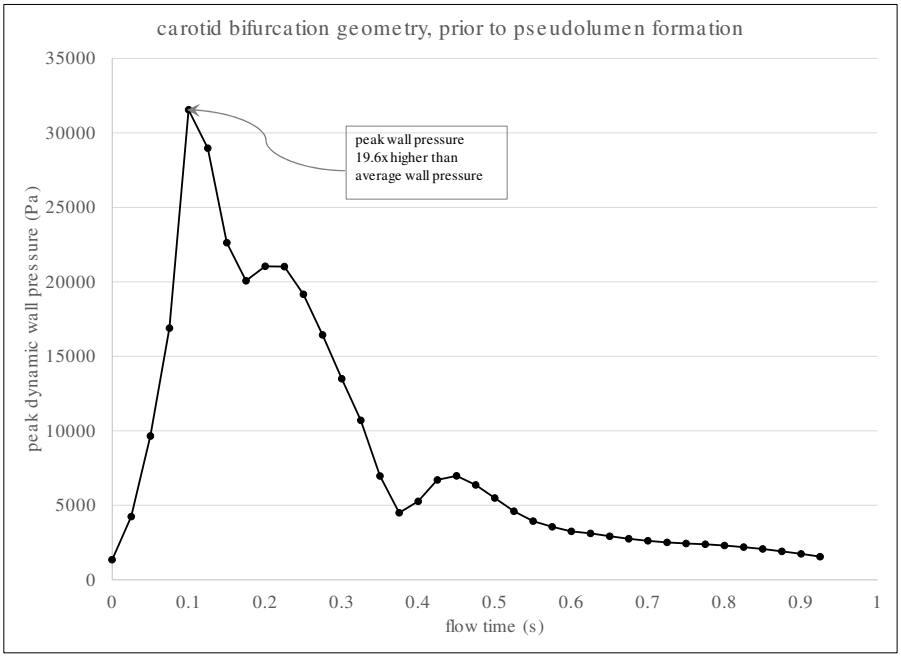

Fig. S2. Peak dynamic pressure along the wall of the geometry at each timestep of the cardiac cycle. Interrogating the solution at the height of systole reveals that the peak pressure is 19.6x higher than the average dynamic wall pressure at that timestep.

References

1. Figueroa CA, Marcan M, Khlebnikov R, et al. CRIMSON: Cardiovascular Integrated Modelling and Simulation [Computer software]. Retrieved from http://www.crimson.software.
2. Gharahi H, Zambrano BA, Zhu DC, DeMarco JK, Baek S. Computational fluid dynamic simulation of human carotid artery bifurcation based on anatomy and volumetric blood flow rate measured with magnetic resonance imaging. *Int J Adv Eng Sci Appl Math*. 2016;8:46-60.
3. Gijsen FJ, van de Vosse FN, Janssen JD. The influence of the non-Newtonian properties of blood on the flow in large arteries: steady flow in a carotid bifurcation model. *J Biomech*. 1999;32(6):601-608.
4. Hoi Y, Wasserman BA, Xie YJ, et al. Characterization of volumetric flow rate waveforms at the carotid bifurcations of older adults. *Physiol Meas*. 2010;31(3):291-302.
5. Zhang Y, Furusawa T, Sia SF, Umezu M, Qian Y. Proposition of an outflow boundary approach for carotid artery stenosis CFD simulation. *Comput Methods Biomech Biomed Engin*. 2013;16(5):488-494.

Video legends

Video S1. Ulcerated plaque

Video S2. Ulcerated plaque_wallstress

Video S3. Ulcerated plaque_dynamicpressure

Video S4. Shallow and deep excavations

Video S5. Excavation_wallstress

Video S6. Excavation_dynamicpressure

Video S7. False Lumen Formation

Video S8. FLF_dynamicpressure

Video S9. FLF_wallstress

Video S10. Complete occlusion by thromboatheroma

Video S11. Critical stenosis_dynamicpressure

Video S12. Critical stenosis_wallstress

Video S13. Shallow excavation_pathline

Video S14. Deep excavation_dynamicpressure

Video S15. Deep excavation_pathline

Video S16. String sign_pathline